FULL TITLE
*ASP Conference Series, Vol. **VOLUME**, **YEAR OF PUBLICATION***
NAMES OF EDITORS

Mass transfer in eccentric binaries using the binary evolution code `BINSTAR`

P. J. Davis, L. Siess, R. Deschamps

Institut d'Astronomie et d'Astrophysique, Université Libre de Bruxelles (ULB), CP 226, Boulevard du Triomphe, Brussels, Belgium

Abstract. Using our state-of-the-art binary evolution code `BINSTAR`, we calculated mass transfer rates via Roche lobe overflow for a $1.50 + 1.40$ M$_\odot$ main sequence binary system with an eccentricity of 0.25 and orbital period of approximately 0.7 d. The impact of an eccentric orbit, and an asynchronously rotating donor star on the Roche lobe radius is considered, and their effect on the mass transfer rate is investigated.

1. Introduction

The Roche model, which assumes that the orbit is circular and that the donor star is rotating synchronously with the orbital period, is widely applied in the studies of interacting binaries. The justification for these approximations is provided by the short timescales needed to circularize the orbit and synchronize the donor star (Zahn 1977).

However, this model has been challenged by observations, in particular by the Kepler satellite, which has detected 14 systems with eccentricities between 0.5 and 0.85 (see e.g. Dong et al. 2013). Furthermore, evidence of mass transfer in eccentric systems has been reported in the post-AGB system HD 44179 (Witt et al. 2009), BX Mon (Leibowitz & Formiggini 2011) and in the black hole binary HLX-1 (Lasota et al. 2011). From the theoretical point of view, Sepinsky et al. (2007b, 2009) found that mass transfer may act to increase the eccentricity on a shorter timescale than the tidal timescale which acts to decrease it.

Hence, the Roche model cannot be justified in such systems. Indeed, the rotation of the donor and the eccentricity of the orbit will modify the donor's Roche lobe radius (Sepinsky et al. 2007a), in turn affecting the mass transfer rate. These effects were not accounted for by the standard Eggleton (1983) formalism.

Here, we present calculations of mass transfer for a main sequence binary system consisting of a donor star of mass $M_1 = 1.50$ M$_\odot$ and an accretor of mass $M_2 = 1.40$ M$_\odot$. Their radii are $R_1 \approx 1.4$ R$_\odot$ and $R_2 \approx 1.2$ R$_\odot$, respectively. They have an age of approximately 1.3 Gyr, and a metallicity of $Z = 0.001$. We use a mixing length parameter of $\alpha_{\rm MLT} = 1.71$, and convective overshooting is not considered. The eccentricity is $e = 0.25$ and the semi-major axis $a = 4.80$ R$_\odot$.

In §2, we describe the `BINSTAR` code, and the key input physics. Calculated mass transfer rates, and the effect of eccentricity, rotation and deformation of the donor due to tides and spin are presented in §3. We also discuss the extent

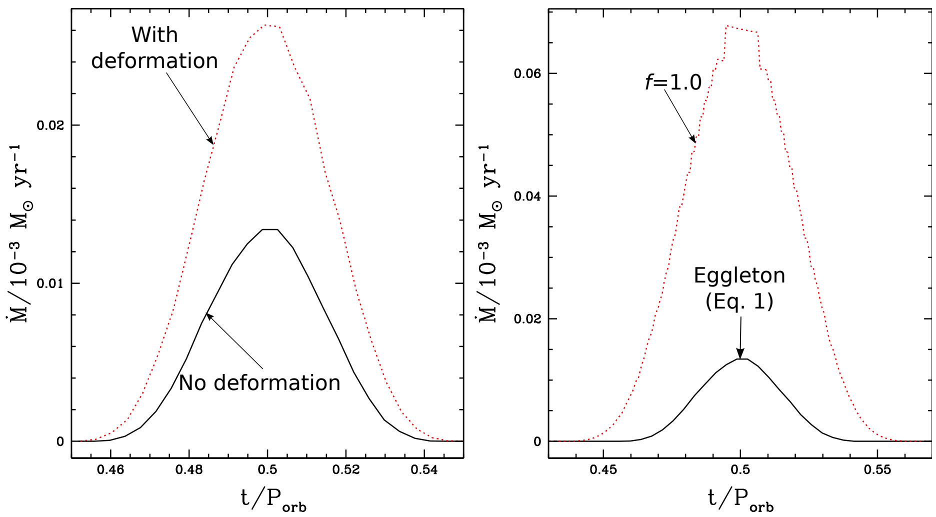

Figure 1. **Left:** evolution of the mass transfer rate, $\dot{M}$, with time since apastron, in units of $P_{\rm orb}$, with (dotted, red curve) and without (solid, black curve) tidal and rotational deformation of the donor. **Right:** The same as the left panel, but where the Roche lobe radius has been calculated using Eq. (1) (solid curve), or using Eq. (2) with $f = 1.0$ (i.e. synchronous rotation of the donor, dotted curve).

to which mass transfer is expected to be conservative is discussed in §4, before summarizing our results in §5. Further details of this study can be found in Davis et al. (2013, in press).

2. Computational Method

`BINSTAR` is an extension of the 1-dimensional, single star evolution code `STAREVOL` (see Siess 2010, and references therein), and is primarily designed for the evolution of low- to intermediate-mass binaries. `BINSTAR` simultaneously solves for the stellar structure equations of each star, and for the orbital separation and eccentricity. `BINSTAR` can also handle semi-convection, thermohaline mixing and diffusive overshooting, and contains a nuclear network of 53 species up to ^{37}Cl. For further details of the binary input physics, see Siess et al. (2013).

2.1. Roche lobe radius

For a binary system where the instantaneous orbital separation is D, and the donor star is assumed to be in synchronous rotation, its Roche lobe radius is accurately given by the Eggleton (1983) formula

$$R_{\mathcal{L}_1} = \frac{0.49q^{2/3}}{0.6q^{2/3} + \ln(1+q^{1/3})} D, \qquad (1)$$

where the mass ratio $q = M_1/M_2$.

To account for the effect of the eccentricity of the orbit and the rotation of the donor, we follow the formalism described by Sepinsky et al. (2007a), that gives the Roche potential (normalized to the gravitational potential of the accretor) as

$$\Psi = -\frac{q}{(x^2+y^2+z^2)^{\frac{1}{2}}} - \frac{1}{[(x-1)^2+y^2+z^2]^{\frac{1}{2}}} - \frac{1}{2}\frac{f^2(1+e)^4}{(1+e\cos\nu)^3}(1+q)(x^2+y^2)+x. \tag{2}$$

Here, the x-axis lies along the line joining the centers of mass of the two stars, in the direction from the donor to the accretor, the z-axis is perpendicular to the plane of the orbit and is parallel to the spin angular velocity of the donor, and the y-axis is perpendicular to the x-axis, and completes a right-handed coordinate set. All coordinates are given in units of D.

If $x_{\mathcal{L}_1}$ is the distance (in units of D) from the centre of mass of the donor to the inner-Lagrangian point (where $\partial\Psi/\partial x = 0$), then the Roche potential, $\Psi_{\rm R}$, is found by setting $x = x_{\mathcal{L}_1}$, $y = 0$ and $z = 0$ in Eq. (2). The volume enclosed by the surface, $\Psi = \Psi_{\rm R}$, is calculated using a 32-point Gaussian quadrature technique. Therefore, $R_{\mathcal{L}_1}$ is defined as the radius of a sphere with the same volume as the Roche lobe. In Eq. (2) f is the spin angular speed of the donor star in units of the orbital angular speed at periastron, i.e.

$$f = \frac{\Omega_1}{\omega_{\rm peri}}. \tag{3}$$

Hence, $f < 1$ indicates that the donor is rotating sub-synchronously at periastron, $f = 1$ signifies synchronous rotation, while $f > 1$ indicates super-synchronous rotation.

2.2. Calculating mass transfer rates

If mass is lost from the optically thin layers of the donor star, then the mass transfer rate, $\dot{M}$, is calculated using the scheme described by Ritter (1988). However, this formalism only applies if $R_{\mathcal{L}_1}$ and R_1 evolve in step. If this is not the case, mass may be removed from the deeper, optically thick layers. In this instance, $\dot{M}$ is determined using the Kolb & Ritter (1990) formulation. In either case, $\dot{M}$ is a function of the amount that the donor star overfills its Roche lobe, i.e.

$$\dot{M} \propto \Delta R, \tag{4}$$

where $\Delta R \equiv R_1 - R_{\mathcal{L}_1}$.

2.3. Tidal and rotational deformation

The deformation of the stellar structure due to tidal and rotational forces follows the formalism described by Landin et al. (2009) and Song et al. (2009). Their method uses the technique developed by Kippenhahn & Thomas (1970), and subsequently improved by Endal & Sofia (1976), that solves the stellar structure equations on equipotential surfaces.

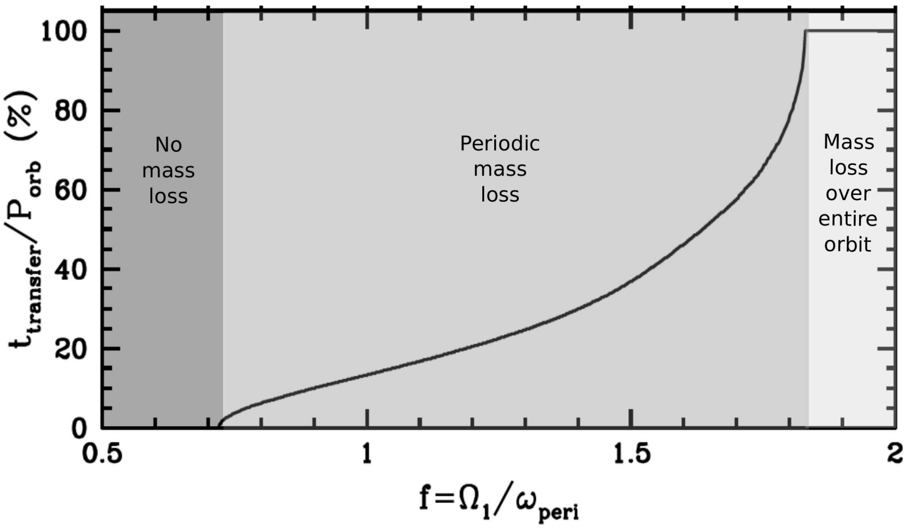

Figure 2. Duration of mass transfer, $t_{\rm transfer}$, in units of $P_{\rm orb}$ as a function of f. The dark grey region indicates that for the corresponding values of f, mass transfer never occurs, medium grey indicates that mass transfer occurs periodically (mainly near periastron), while light gray indicates that mass transfer occurs over the entire orbit.

3. Duration and rates of mass transfer

The solid curve in the left panel of Fig. 1 shows the evolution of $\dot{M}$, where Eq. (1) has been used to calculate the donor's Roche lobe radius. As the stars approach periastron ($t/P_{\rm orb} = 0.5$), $R_{\mathcal{L}_1}$ shrinks as D declines (Eq. 1), causing a corresponding rise in the amount that the star overfills its Roche lobe, and therefore in $\dot{M}$ (Eq. 4). The mass transfer rate reaches a maximum value of about 1.3×10^{-5} $M_\odot$ yr^{-1}. The reverse process occurs as the stars move away from periastron. The evolution of $\dot{M}$ has a Gaussian-like profile, in agreement with the smooth-particle hydrodynamics (SPH) calculations of Lajoie & Sills (2011).

If the deformation of the donor's structure due to tides and rotation is taken into account, the mass transfer rate is enhanced by about a factor of 3 (Fig. 1, left panel, dotted curve), because the donor's radius is larger as a result of its lower surface gravity.

The right panel of Fig. 1 shows that if we take into account the effects of eccentricity and rotation for the determination of the Roche radius (with $f = 1.0$ for synchronous rotation), the value of $\dot{M}$ at periastron is about a factor of 7 larger than the 'standard' value when using Eq. (1). This is because Eggleton's formula gives a larger value for the Roche lobe radius than the one derived from the effective potential (Eq. 2).

For a fixed value of the eccentricity, the donor's rotation will also impact on the duration of mass transfer, $t_{\rm transfer}$ (Fig. 2), via the parameter f in Eq. (2). We find that if $f \lesssim 0.7$ mass transfer never occurs because the Roche lobe

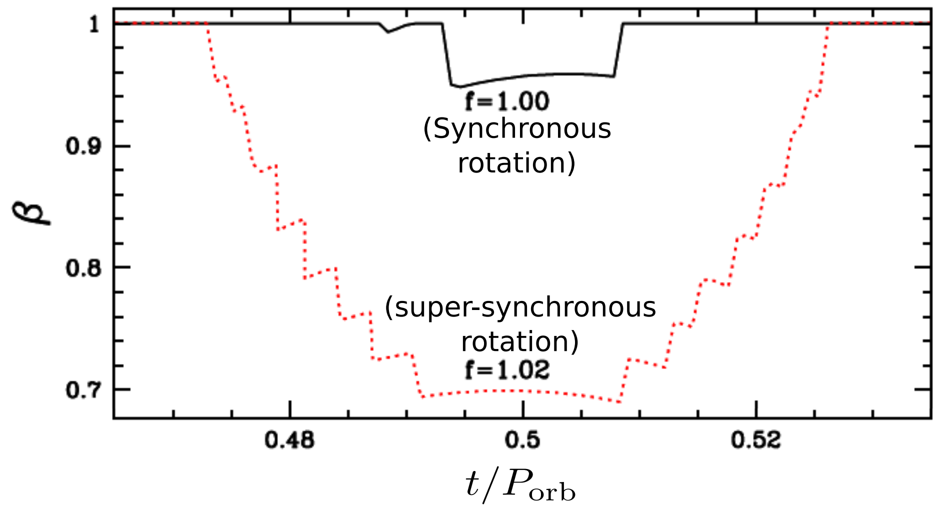

Figure 3. Evolution of the parameter $\beta = |\dot{M}_2/\dot{M}_1|$, for the case where the donor is rotating synchronously with the orbit at periastron ($f = 1.0$, black curve), and super-synchronously ($f = 1.02$, dotted curve).

radius is too big for the donor to fill it, even at periastron. On the other hand, for $0.7 \lesssim f \lesssim 1.8$, mass transfer occurs over a part of the orbit, mainly near periastron, while for $f \gtrsim 1.8$, the Roche lobe radius is sufficiently small such that mass transfer occurs over the entire orbit.

4. Mass ejection from the accretor

For our binary configuration, we find that mass directly impacts the surface of the accretor. This causes a local increase in temperature and luminosity, termed *hotspot*. If $\dot{M}$ is higher than some critical value, $\dot{M}_{\rm crit}$, then the hotspot luminosity will exceed the Eddington value, $L_{\rm Edd}$, allowing for mass ejection. To explore this possibility, we implemented in `BINSTAR` the hotspot formalism described by van Rensbergen et al. (2008) to calculate $\dot{M}_{\rm crit}$.

Fig. 3 shows the evolution of the accretion efficiency, β, defined as the ratio of the mass loss rate from the donor to the mass accretion rate of the gainer. Values of $\beta < 1$ indicate non-conservative mass transfer, and occurs when $f \gtrsim 1$. Since increasing f enhances $\dot{M}$ (§3), raising the angular speed of the donor drives the value of $\dot{M}$ ever further above $\dot{M}_{\rm crit}$. In turn, this leads to a higher hotspot luminosity and a greater rate of mass ejection from the accretor. During one orbit, the total ejected mass from the accretor is about 10^{-9} M$_\odot$ for the synchronous model, and 2×10^{-8} M$_\odot$ for the super-synchronous model. Note that due to the modulation of $\dot{M}$ with orbital phase, β reaches a minimum at periastron. The saw-tooth behaviour of β is an artifact due to the insufficient numerical resolution of the donor's surface layers, and is not a physical feature.

5. Summary

For the first time, we have calculated mass transfer in eccentric systems using our state-of-the-art stellar binary evolution code BINSTAR. We find that the evolution of the mass transfer rate has a Gaussian-like profile, with a maximum value attained at periastron, in agreement with SPH simulations. The rate is also significantly enhanced by the tidal and rotational deformation of the donor star. We point out that mass transfer at periastron is a promising mechanism for eccentricity generation in Barium stars (e.g. Soker 2000).

Finally, the eccentricity and the donor's rotation have a significant impact on both the duration and the rate of mass transfer. Increasing the donor's angular speed increases both the duration and rate of mass transfer. If the donor is rotating too slowly, then mass transfer may not occur.

Acknowledgments. PJD is a Chargé de Recherche (FNRS-F.R.S.), RD acknowledges support from the Communauté française de Belgique – Actions de Recherche Concertées and LS is an FNRS Researcher.

References

Davis, P. J., Siess, L., & Deschamps, R. 2013, ArXiv e-prints. 1305.6092
Dong, S., Katz, B., & Socrates, A. 2013, ApJ, 763, L2. 1201.4399
Eggleton, P. P. 1983, ApJ, 268, 368
Endal, A. S., & Sofia, S. 1976, ApJ, 210, 184
Kippenhahn, R., & Thomas, H.-C. 1970, in IAU Colloq. 4: Stellar Rotation, edited by A. Slettebak, 20
Kolb, U., & Ritter, H. 1990, A&A, 236, 385
Lajoie, C.-P., & Sills, A. 2011, ApJ, 726, 67
Landin, N. R., Mendes, L. T. S., & Vaz, L. P. R. 2009, A&A, 494, 209. 0904.2535
Lasota, J.-P., Alexander, T., Dubus, G., Barret, D., Farrell, S. A., Gehrels, N., Godet, O., & Webb, N. A. 2011, ApJ, 735, 89. 1102.4336
Leibowitz, E. M., & Formiggini, L. 2011, MNRAS, 414, 2406. 1102.4458
Ritter, H. 1988, A&A, 202, 93
Sepinsky, J. F., Willems, B., & Kalogera, V. 2007a, ApJ, 660, 1624. arXiv:astro-ph/0612508
Sepinsky, J. F., Willems, B., Kalogera, V., & Rasio, F. A. 2007b, ApJ, 667, 1170. 0706.4312
— 2009, ApJ, 702, 1387. 0903.0621
Siess, L. 2010, A&A, 512, A10
Siess, L., Izzard, R. G., Davis, P. J., & Deschamps, R. 2013, A&A, 550, A100
Soker, N. 2000, A&A, 357, 557. arXiv:astro-ph/0002128
Song, H. F., Zhong, Z., & Lu, Y. 2009, A&A, 504, 161. 0907.4460
van Rensbergen, W., De Greve, J. P., De Loore, C., & Mennekens, N. 2008, A&A, 487, 1129. 0804.1215
Witt, A. N., Vijh, U. P., Hobbs, L. M., Aufdenberg, J. P., Thorburn, J. A., & York, D. G. 2009, ApJ, 693, 1946. 0812.2893
Zahn, J.-P. 1977, A&A, 57, 383